Int. J. Electrochem. Sci., 9 **(2014)** 3864 - 3875

International Journal of
ELECTROCHEMICAL
SCIENCE
www.electrochemsci.org

Impedance Spectroscopy and Dielectric Properties of Silver Incorporated Indium Sulfide Thin Films

Nurdan Demirci Sankır[*], *Erkan Aydın, Mehmet Sankır*

Department of Materials Science and Nanotechnology Engineering, TOBB University of Economics and Technology, Ankara, Turkey
[*]E-mail: nsankir@etu.edu.tr

Received: 2 March 2014 / *Accepted:* 20 March 2014 / *Published:* 14 April 2014

In this study, silver incorporated indium sulfide (In_2S_3) thin films have been deposited on soda lime glass via spray pyrolysis technique. Structural and electrical properties have been tailored by adding controlled amount of silver acetate into the precursor solution. A phase shift form cubic β-In_2S_3 to $AgInS_2$ has been evidenced from X-ray diffraction spectra (XRD). Molecularity of the samples, meaning (Ag+In)/S ratio, has directly affected the electrical conductivity as well as the dielectric properties. Direct and alternating current conductivities increased with increasing the (Ag+In)/S ratio upto 10% silver incorporation. When the silver amount further increased conductivity decreased due to the pronounced secondary phase formation. The complex impedance analysis was used to determine the effect of silver on the conduction mechanism. It has been observed that frequency exponent of all samples were greater than unity indicating the nanocrystalline nature of the films. The variation of dielectric properties and ac conductivity with frequency revealed that the relaxation process in silver incorporated In_2S_3 thin films was due to the Maxwell–Wagner type of interfacial polarization in general.

Keywords: Spray pyrolysis, indium sulfide, silver incorporation, impedance spectroscopy, dielectric properties

1. INTRODUCTION

Indium sulfide (In_2S_3) is a promising material for optoelectronic and photovoltaic applications due to its proper band gap energy, stability and photoconductive nature [1]. Thin films of In_2S_3 have also been gaining more attention as a non-toxic and effective alternative of the cadmium sulfide most commonly used n-type semiconductor for commercial solar cells [2]. Various manufacturing techniques have been used to deposit In_2S_3 thin films such as atomic layer deposition, close space evaporation, electrodeposition, chemical bath deposition, spray-ILGAR, and spray pyrolysis [3-8]. Wet chemical techniques have the advantages of low manufacturing cost, ease of scalability over large

areas and compatibility with various substrates including plastic and even paper. Recently B. Mari et al. reported the electrochemical deposition of the In_2S_3 using an organic solvent, which had the advantages of high boiling point, dielectric constant that allows the solubility of salts and chalcogen precursors in elemental state [9]. In this study, due to its simplicity and very high manufacturing speed spray pyrolysis technique was used to build In_2S_3 thin films. Moreover, this technique does not require expensive solid sources and offers very low solution consumption for large area manufacturing, which are the key factors for the commercialization in the solar cell area. Doping of functional thin films, which is an effective way of tailoring electrical, structural and optical properties, can be easily done by adding the salt of desired element during the spray process. Although, there are numerous works on doping of spray-pyrolyzed oxides such as zinc oxide, nickel oxide and titanium dioxide in literature, there are very limited studies on doping of spray pyrolyzed In_2S_3 thin films [10-13]. Previously, M. Mathew et al. reported the zinc incorporation of the indium sulfide thin films deposited via spray pyrolysis [13]. They claimed that tin doping modified the band gap and electrical properties of the In_2S_3 films favorably over wider ranges making these films suitable for optoelectronic applications. Here, we investigated the structural, optical, electrochemical and dielectric properties of the silver doped spray-pyrolyzed In_2S_3 thin films. According to our best knowledge, this is the first report on effects of silver incorporation on the impedance spectroscopy and dielectric properties of spray pyrolyzed In_2S_3 thin films.

2. EXPERIMENTAL

Silver incorporated In_2S_3 thin films were prepared on soda lime glass using SonoTek FlexiCoat USP coating system. Indium (III) chloride ($InCl_3$, Sigma-Aldrich), and thiourea (NH_2CSNH_2, Sigma-Aldrich) were used as indium and sulfur source, respectively. Silver incorporation was done by adding silver acetate ($Ag(CH_3COO)$, Merck) to the precursor solution at various molarities. Detailed information about the spray pyrolysis system and the silver incorporation was reported in our previous studies [14-16]. The surface morphology of the films was investigated by FEI, Quanta 200 FEG SEM. EDX microanalysis has been used to evaluate the chemical compositions of the films. The optical transmittance spectra of the samples were measured by a Perkin Elmer 600 S UV–VIS spectrophotometer in wavelength range of 200-800 nm. Room temperature AC conductivity of the films was performed using Solartron SI 1260 Impedance/Gain-Phase Analyzer equipped with a 1296 Dielectric Interface. Impedance data were taken in dark conditions at room temperature using the AC modulation voltage of 500 mV at 1 Hz -1 MHz frequency range. Data fitting and analysis of the electrical impedance measurements were done using Z-View software (Scribner Associates).

3. RESULTS AND DISSCUSSIONS

3.1. Structural and Optical Properties

In order to investigate the effect of silver incorporation on the film properties, various amounts of silver acetate have been added into the precursor solution. 10 mM of indium concentration was kept

constant for all experiments, which was assumed as 100 %. Then, silver to indium molar ratio ([Ag]:[In]) was defined as percent silver concentration of indium concentration. Figure 1 depicts the SEM images of the silver incorporated In_2S_3 thin films. As can be seen in this figure, all of our films were homogenous and crack free. Moreover, silver addition did not affect the surface morphology of spray-pyrolyzed In_2S_3 thin films. EDX analysis, carried out at accelerating voltage of 15 kV and spot size 3μm, has been performed to determine the chemical composition of the In_2S_3 thin films.

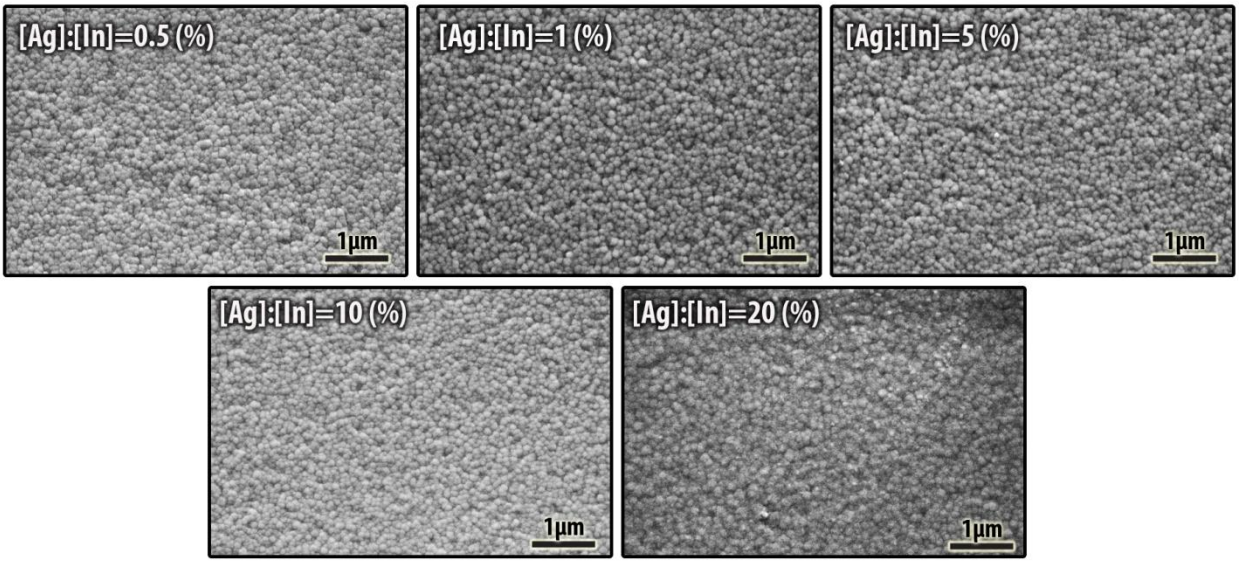

Figure 1. SEM micrographs of in-situ Ag doped In_2S_3 films.

As targeted, the silver amount in the films increased with increasing the molarity of the silver acetate. Figure 2 (b) shows the variation of the elements in atomic percent determined from EDX analysis for various silver concentrations. It has been observed that sulfur atomic percent in the films did not changed drastically with silver incorporation. On the other hand, indium percent decreased while silver percent in the films increased. This indicated the possibility of sitting of the silver atom in the cationic sites of In_2S_3 structure. Silver incorporation to the films was also detected from the visual appearance of the films. As can be seen in Figure 2 (a), color of the films was changed from light yellow to orange in daylight with silver incorporation. Besides, the atomic ratio of (Ag+In)/S for all samples have been calculated using EDX results and listed in Table 1. Although there were some fluctuations, (Ag+In)/S ratio increased with increasing the silver concentration in the precursor solution. This ratio can be an indication of phase shift towards In_2S_3 to $AgInS_2$. Also the total ratio of metals to sulfur in the films may effect the electrical conduction. Besides, EDX analysis confirmed the chlorine contamination most probably from the usage of chlorine based salts as precursor chemical (Fig. 2(b)). The chlorine percent in the films increased from 10.1 to 11.5 at. % with increasing the silver concentration. This was a strong indication of formation of chlorine and silver based secondary phases with increasing the [Ag]:[In].

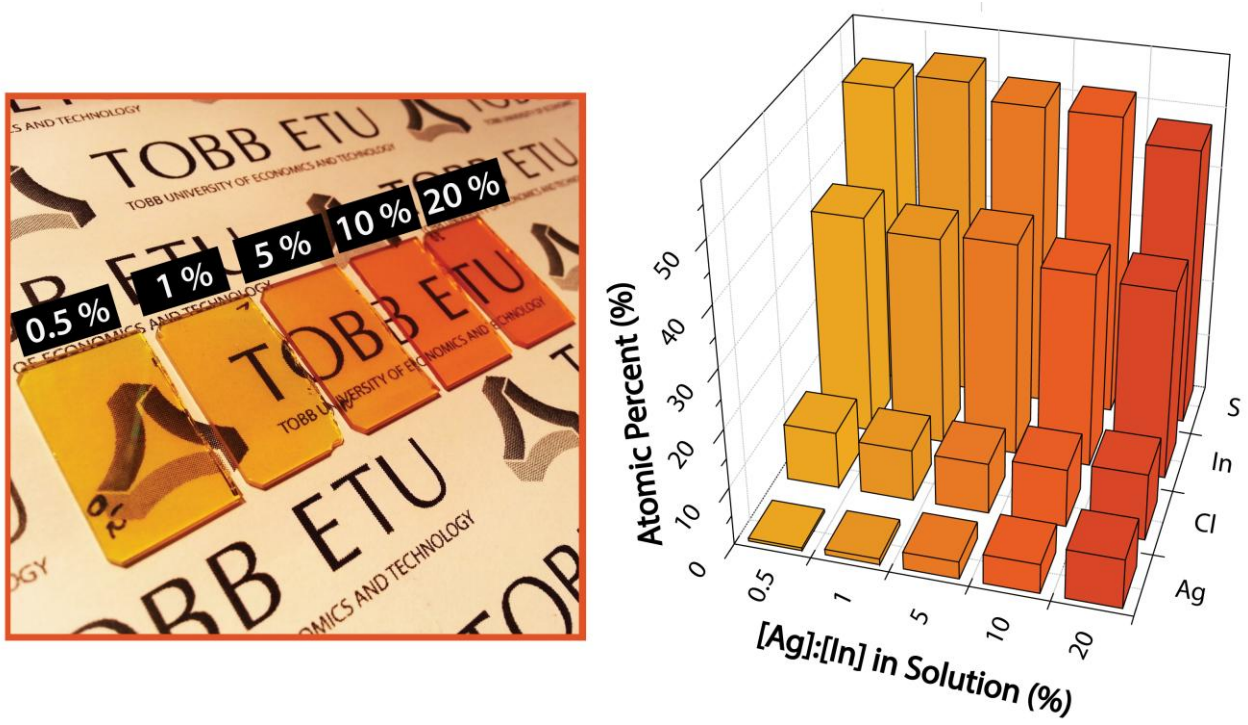

(a) **(b)**

Figure 2. (a) Visual appearance and **(b)** atomic ratios of silver incorporated In_2S_3 films

Table 1. Mean crystallite size, band gap and dc conductivity of the silver incorporated In_2S_3 thin films

$[Ag^+]:[In^{3+}]$ (%)	(Ag+In)/S	Mean Crystallite Size (nm)	Band Gap (eV)
0.5	0.74	40	2.75
1	0.68	30	2.76
5	0.77	46	2.76
10	0.75	44	2.70
20	0.87	44	2.66

Crystal structure of the films has been confirmed via X-ray diffraction analysis. Figure 3 shows the XRD patterns of the samples with various silver concentrations. Quantitative analysis of these patterns showed that the major phase for all our samples was cubic β-In_2S_3 (JCPDS Card No. 32-456). The intensity of the peak around 33° (2θ), could be attributed to the (200) cubic plane, decreased with increasing the silver incorporation. Secondary most intense peak for all samples was located around 28° (2θ) which could be attributed to both (311) cubic β-In_2S_3 or orthorhombic $AgInS_2$ [17, 18]. Therefore, it is possible to mention about a phase shift from cubic β-In_2S_3 to orthorhombic $AgInS_2$ with silver addition. The presence of AgCl crystals was also confirmed from XRD data (JCPDS file no.: 31-1238). The peaks observed around 28, 33, 47° (2θ) could be assigned to both AgCl and cubic In_2S_3 structure.

Spray deposited In_2S_3 films consist of small nano scale crystallites and this probably triggers the formation of secondary phases, which have different compositions. The detailed structural analysis of silver incorporated In_2S_3 thin films have been reported in our previous work [16]. Mean crystallite size has been calculated using Scherrer's formula with 0.89 correction factor. As summarized in Table 1 all of our films were in nanocrystalline nature. Previously similar crystallite sizes have been reported for the wet chemical deposition of In_2S_3 thin films [13].

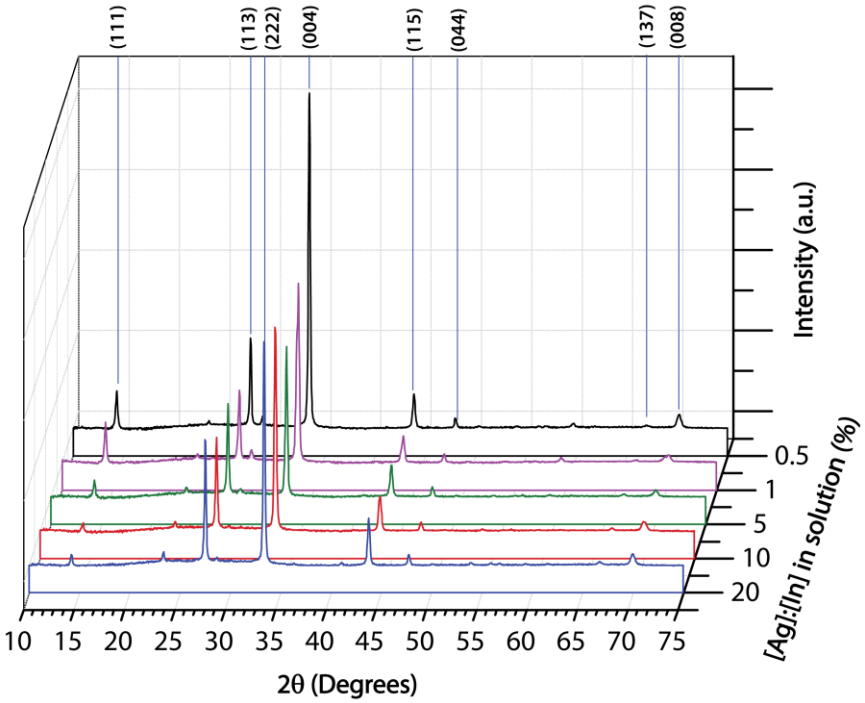

Figure 3. XRD spectra of In_2S_3 thin films with various silver incorporation

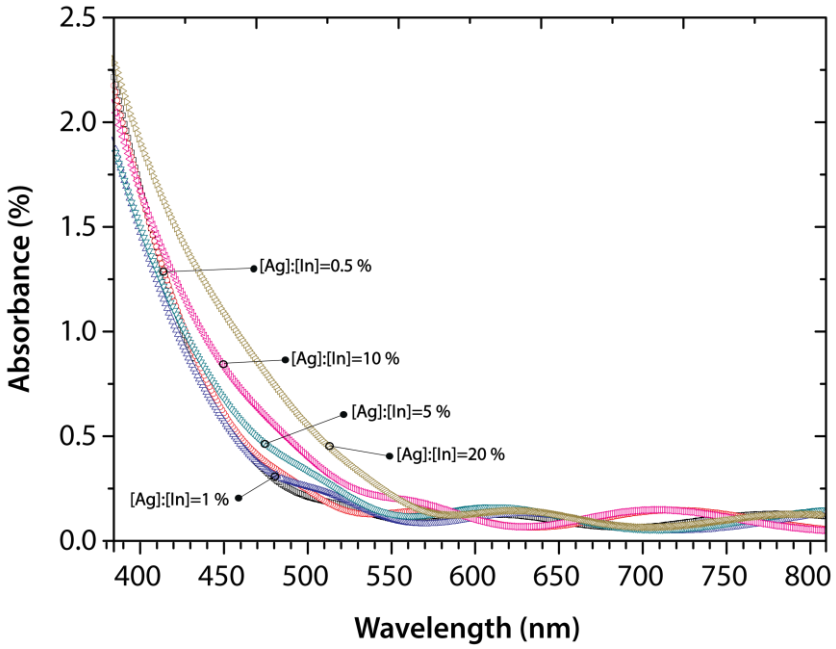

Figure 4. Absorbance versus wavelength spectra of the silver doped In_2S_3 thin film.

Optical properties of the silver incorporated In_2S_3 has been observed form the UV-VIS spectra of the thin films (Fig. 4). The absorbance of thin films increased with silver addition. As can bee seen in Table 1, band gap energies of the films, which have been calculated using the UV-VIS data, decreased from 2.75 to 2.66 eV by silver addition. All these values were proper for using these films as the window layer for solar cell applications. It can also be concluded that the in-situ silver doping could be used to tailor the optical properties of the In_2S_3 films.

3.2 Impedance Spectroscopy

Frequency dependent electrical conductivity measurements of the silver incorporated In_2S_3 thin films have been performed at room temperature, under dark and in the frequency range of 1Hz-1 MHz. Frequency dependant impedance data have been recorded using Solartron SI 1260 Impedance/Gain-Phase Analyzer equipped with a 1296 Dielectric Interface. Figure 5 shows the Nyquist plots of our samples. For all samples single semicircle fit was observed indicating the single relaxation process. Equivalent circuit can also be seen in inset Figure 5. Circuit parameters have been calculated from the fitting values obtained via Z-View software and summarized in Table 2. As expected, R_s value which indicates the contact resistances were comparable for all of our samples and were in the range of kilo ohm. The bulk resistances of the samples (R_p) were in consistent with conductivity of the films and as a general trend decreased with increasing the (Ag+In)/S ratio in the films. As can be also seen in Table 2, there was no significant change in capacitance with silver incorporation. C_p of the samples was around 1.5 pF for all samples. Bode and phase angle diagrams of the silver doped In_2S_3 thin films can bee seen in Figure 5.

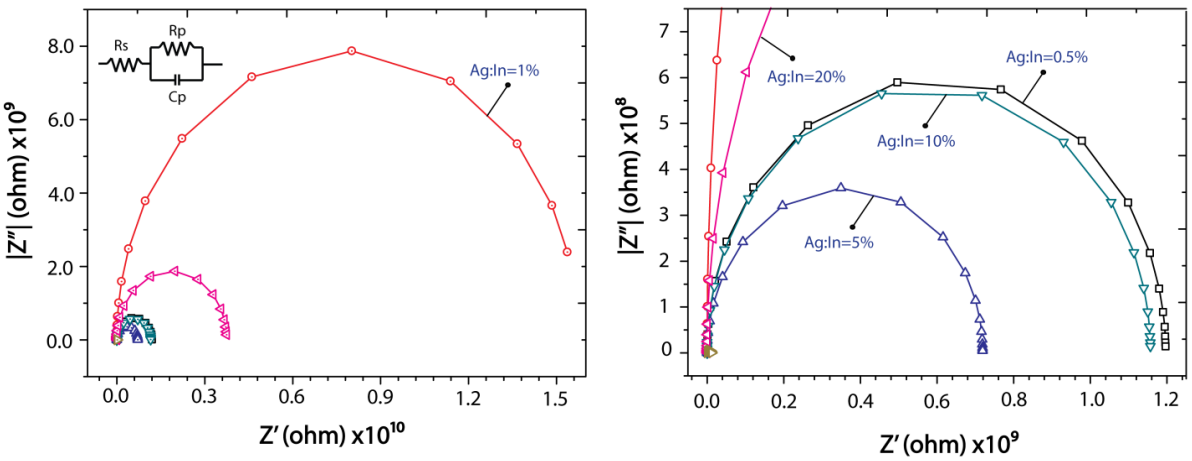

Figure 5. Nyquist plots of silver incorporated In_2S_3 films for various [Ag]:[In] concentrations in solution.

The analysis of Bode plots (Fig. 6) gave information complementary to the one obtained from Nyquist plots. One time constant behavior can be also seen in these diagrams. Moreover, samples having more silver showed higher capacitive arc.

Table 2. Direct current (dc) conductivity and equivalent circuit parameters of

[Ag]:[In] (%)	σ_{dc} (S/cm)	R_s (Ω)	R_p (Ω)	C_p (F)
0.5	$1.5x10^{-5}$	$8x10^{3}$	$1.2x10^{9}$	$1.6x10^{-12}$
1	$0.6x10^{-5}$	$8x10^{3}$	$1.6x10^{10}$	$1.6x10^{-12}$
5	$2.8x10^{-5}$	$8x10^{3}$	$0.7x10^{9}$	$1.4x10^{-12}$
10	$1.6x10^{-5}$	$7x10^{3}$	$1.1x10^{9}$	$1.7x10^{-12}$
20	$0.7x10^{-5}$	$7x10^{3}$	$3.9x10^{9}$	$1.6x10^{-12}$

Figure 6 also reveals that parallel R-C circuit can used to explain alternating current measurements of our samples. We observed one plateau at low frequencies in logZ versus logf plots and two plateaus in phase angle graphs due to relatively very small R_s compare to the R_p. Furthermore, the resistance values can be observed from low frequency intercept in Bode plots were consistent with the conductivity of our thin films.

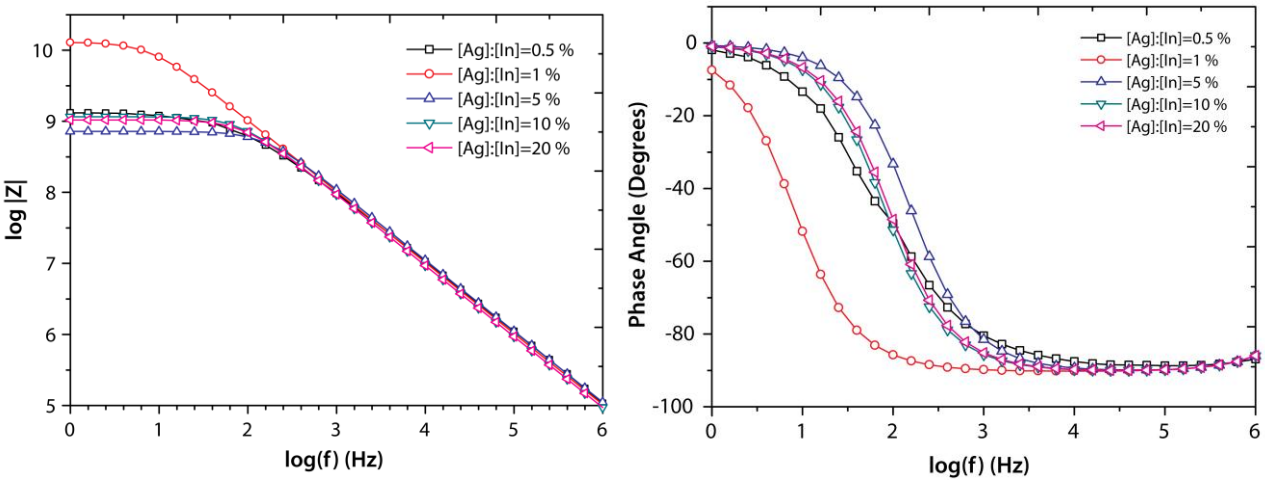

(a) **(b)**

Figure 6. (a) Bode and **(b)** phase angle graphs of silver doped In_2S_3 thin films

The electrical conductivity σ(ω) of the silver incorporated In_2S_3 thin films at a particular temperature over a frequency range can be written in the combination of DC and AC part;

$$\sigma(\omega) = \sigma_{dc} + A\omega^{s} \qquad (1)$$

where σ_{dc} is the DC part of the electrical conductivity, A is the temperature dependant constant and s is the frequency exponent. Figure 7 shows the change in σ_{ac} with frequency. For all samples, the conductivity increases sharply with frequency showing a distinct change in slope. This linear region at

ln σ_{ac} versus lnω graphs started at different cut-off frequencies, which was in the range of 400-800 Hz. Below and under these limits, conductivity stayed constant. Stability of the conductivity can be attributed to the free charge formation in the film. Moreover, the increase in the conductivity with frequency could be a sign of release of trapped charges in the disorder system. This is consisted with the nanocrystalline nature of spray-pyrolyzed films. It was also observed that AC conductivity of the silver incorporated films were comparable with each other. The frequency exponent "s" of the silver incorporated In_2S_3 thin films have been calculated using the slope of ln σ_{ac} versus lnω plots. "s" is roughly treated as constant less than 1 and often used to describe the ac component contributing to the dispersive region [19]. In our study "s" is greater than unity and decreasing from 1.9 to 1.5 by increasing the silver amount. It has been known that "s" can hold value greater than unity in some mixed compounds, like $(NH_4)_3H(SO_4)_{1.42}(SeO_4)_{0.58}$ and polymeric networks [20, 21]. This high "s" value most probably was due to the distribution of accessible conduction paths stemming from the absence of periodicity in space and the presence of defects [21].

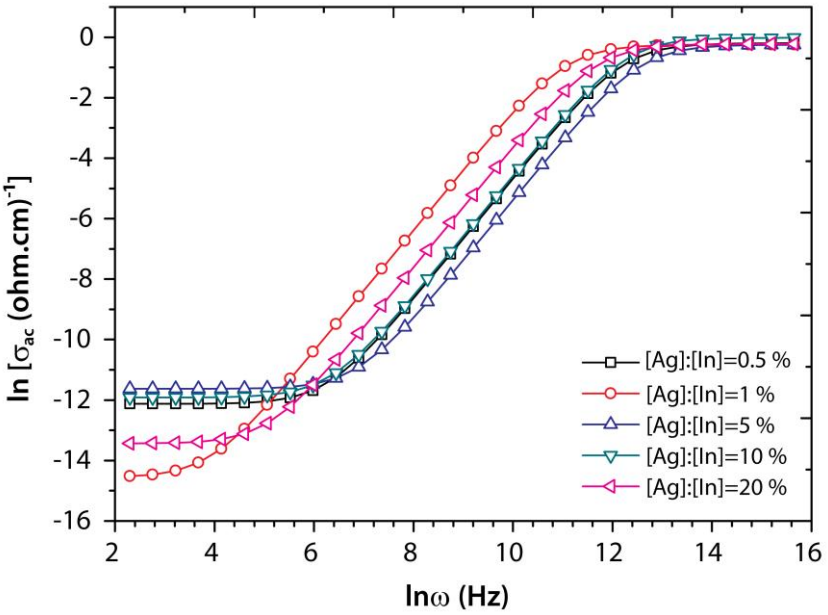

Figure 7. Frequency dependence of σ_{ac} of In_2S_3 films for different $[Ag^+]$:$[In^{3+}]$ concentrations in solution.

3.3 Dielectric Properties

The frequency dependence of the dielectric permitivity (ε') of silver incorporated In_2S_3 thin films at room temperature can be seen in Figure 8. It has been observed that all of the samples exhibited relatively high dielectric permitivity at low frequencies and it decreased with increasing the frequency. In the high frequency range dielectric constant were independent of silver amount and frequency. Previously M. A. M. Seyam has reported a similar behavior for the In_2S_3 thin films deposited via thermal evaporation method [22].

The decrease in dielectric permitivity with frequency can be attributed to the contribution of the multicomponent polarizability, which are deformational and relaxation. Deformational polarizability is the mutual displacement of the oppositely charged partciles under the action of applied field. On the other hand, the relaxation plorizability originated from limited mobility of the permenant dipoles shows up at lower frequencies. In other words, as the frequency increased dipoles will no longer be able to rotate sufficiently, so that their oscillation will begin to lag behind those of the field. Hence dielectric constant at high frequencies approaches a limit value [23].

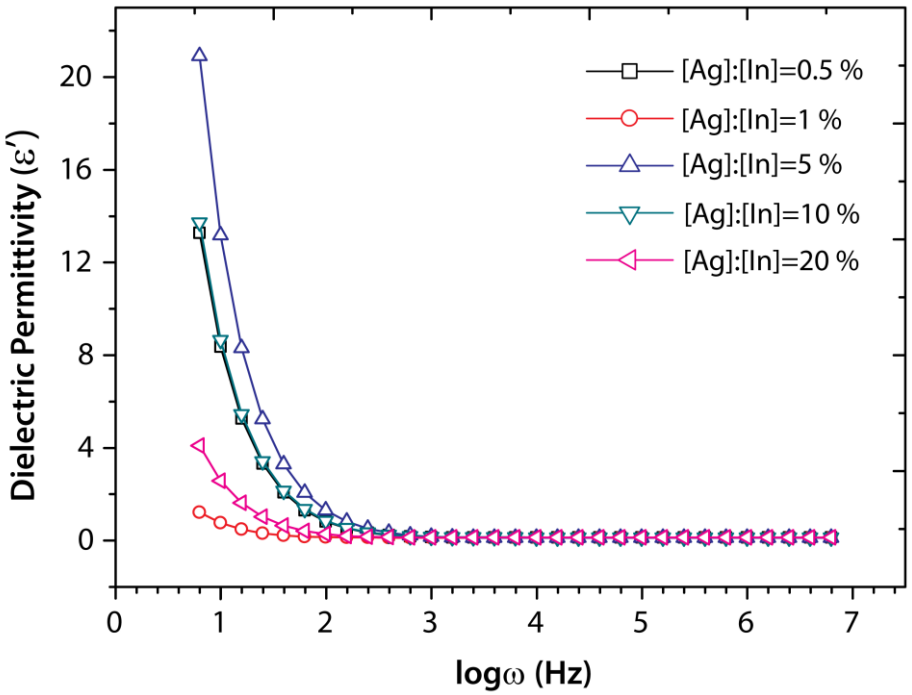

Figure 8. log(ω)-ε plots of in-situ Ag doped In_2S_3 films for different $[Ag^+]$:$[In^{3+}]$ concentrations in solution.

The electrical modulus (*M*), which is defined as the reciprocal of the complex relative permittivity, can be used to understand electrical relaxation processes. *M* corresponds to the relaxation of the electric field in the material when the electric displacement remains constant [24]. Figure 9 shows the variation of the real and imaginary part of electrical modulus as a function of logarithmic angular frequency, which can be calculated using the following equations;

$$M^* = \frac{1}{\varepsilon^*} = M' + jM'' \qquad (2)$$

The real and the imaginary part of M^* are given as;

$$M' = \frac{\varepsilon'}{\varepsilon'^2 + \varepsilon''^2}$$
$$M'' = \frac{\varepsilon''}{\varepsilon'^2 + \varepsilon''^2} \qquad (3)$$

At relatively lower frequencies M' tends to be constant for all samples. Also, similar behavior has been observed at the high frequencies. Figure 9 (b) depicts an asymetric behavior with respect to a peak maxima, whose positions were frequency dependent. Moreover maxima of M'' shifted through higher frequencies with increasing the (Ag+In)/S ratio upto 20% silver loading. For the 20% [Ag]:[In] sample, M''_{max} shifted back. The analomoous behavior of 20% silver contaning films could be attributed to the crystal phase shift confirmed by XRD analysis. Combined with the dielectric permitivity results it is possible to explain the relaxation process in silver doped In_2S_3 thin films with Maxwell-Wagner polarization. This theorem has been used to explain the effect of large grain boundaries on the electrical conduction mechanism [25]. In this model, the dielectric materials with heterogenic structure are assumed as the systems consisting of conducting grains separated by the resistive grain boundaries. Therefore the grain boundary volume controls the behavior of ε′ at low frequencies. The higher values of dielectric permitivity at low frequencies can be explained on the basis of interfacial space charge polarization due to inhomogeneous dielectric structure.

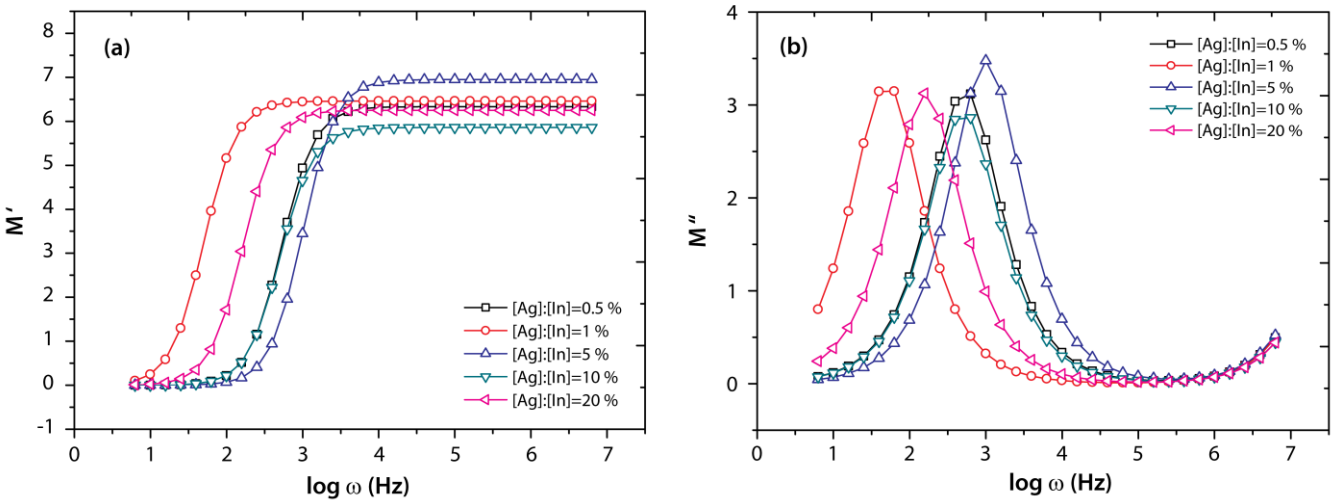

Figure 9. Modulus plots of in-situ Ag doped In_2S_3 films for different $[Ag^+]$:$[In^{3+}]$ concentrations in solution.

4. CONCLUSIONS

With this study for the first time it has been proved that dc and ac electrical properties of spray pyrolyzed In_2S_3 thin films can be tailored via very simple in-situ silver incorporation. In_2S_3 thin films have been deposited soda lime glass at various silver concentrations. EDX results showed that silver amount in the films was increased with increasing the silver concentration in the precursor solution. Optical absorption of the films increased with increasing the silver concentration and therefore band gap energy decreased. Although the silver atomic percent in the films increased with silver concentration (Ag+In)/S ratio fluctuated. This ratio was directly effected the dc conductivity and the all other electrical properties upto 10%. After that point, conductivity of the samples decreased most probably due to the secondary phase formations in the films. XRD analysis revealed that main crystal

structure of all samples was cubic β-In_2S_3. Also all films were in nanocrystalline nature. Secondary phases such as $AgInS_2$ and AgCl have been observed with increased silver amount. XRD analysis combined with EDX results indicated that AgCl phase became pronounced with increasing the silver concentration. This directly affected the electrical properties. In other words, both ac and dc conductivity of the films decreased when the silver incorporation increased to 20%. This also affected the dielectric properties such as dielectric permitivity, modulus and tangent loss. Two different frequency dependencies of dielectric constant at low and high frequency range and also asymmetric modulus behavior indicated that relaxation process in silver doped In_2S_3 thin films can be explained with Maxwell-Wagner polarization.

ACKNOWLEDGEMENTS
This study was supported by Republic of Turkey Ministry of Science, Industry and Technology under the research Grant 01072.STZ.2011-2.

References

1. B. Asenjo, C. Sanz, C. Guillén, A.M. Chaparro, M.T. Gutiérrez, J. Herrero, *Thin Solid Films*, 515 (2007) 6041
2. N. Barreau, *Sol. Energy* 83 (2009) 363
3. S. Spiering, D. Hariskos, M. Powalla, N. Naghavi, D. Lincot, *Thin Solid Films*, 431–432 (2003) 359
4. N. Revathi, P. Prathap, K.T. Ramakrishna Reddy, *Solid State Sci.* 11 (2009) 1288
5. M. Abdel Haleem, M. Ichimura, *Thin Solid Films*, 516 (2008) 7783
6. C.D. Lokhande, A. Ennaoui, P.S. Patil, M. Giersig, K. Diesner, M. Muller, H. Tributsch, *Thin Solid Films*, 340 (1999) 18
7. N. A. Allsop, A. Schonmann, H.-J. Muffler, M. Bar, M. C. Lux-Steiner, Ch.-H. Fischer, *Prog. Photovolt: Res. Appl.* 13 (2005) 607
8. S. Buecheler, D. Corica, D. Guettler, A. Chirila, R. Verma, U. Müller, T.P. Niesen, J. Palm, A.N. Tiwari, *Thin Solid Films*, 517 (2009) 2312
9. B. Mari, M. Mollar, D. Soro, R.Henriquez, R. Schrebler, H. Gomez, *Int. J. Electrochem. Sci*., 8 (2013) 3510
10. M. Mathew, M. Gopinath, C. S. Kartha, K. P.Vijayakumar, Y. Kashiwaba, T. Abe, *Sol. Energy*, 84 (2010) 888
11. J-H. Lee, B-O. Park, *Mater. Sci. Eng. B-Adv.*, 106 (2004) 242
12. P. Puspharajah, S. Radhakrishna, A. K Arof, *J. Mater. Sci.*, 32 (1997) 3001
13. H. Yanagi, Y. Ohoka, T. Hishiki, K. Ajito, A. Fujishima, *Appl. Surf. Sci*., 113-114 (1997) 426
14. E. Aydin, N.D. Sankir, *J. Opt. Adv. Mater.*, 15 (2013) 14
15. N.D. Sankir, E. Aydin, H. Unver, E. Uluer, M. Parlak, *Sol. Energy* 95 (2013) 21
16. E. Aydin, M. Sankir, N. D. Sankir, *Submitted to J. Alloy. Compd*. (2014)
17. T.T. John, C.S. Kartha, K.P. Vijayakumar, T. Abe, Y. Kashiwaba, *Appl. Surf. Sci.*, 252 (2005) 1360
18. S. Lugo, Y. Pena, M. Calixto-Rodriguez, C. López-Mata, M.L. Ramón, I. Gómez, A. Acosta, *App. Surf. Sci.* 263 (2012) 440
19. N.F. Mott, E.A. Davis, *Electronic Processes in Non-Crystalline Materials*, Clarendon Press, Oxford (1979)
20. B. Louati, M. Gargouri, K. Guidara, and T. Mhiri, J. Phys. Chem. Solids 66 (2005) 762

21. A. N. Papathanassiou, I. Sakellis, J. Grammatikakis, *Appl. Phys. Lett.*, 91 (2007) 122911
22. M. A. M. Seyam, A.E. Bekheet, A. Elfalaky, *Eur. Phys. J. AP* 16 (2001) 99
23. F. Carpi, D. D. Rossi, R. Kornbluh, R. Pelrine, P. Sommer-Larsen, *Dielectric Elastomers as Electromechanical Transducers*, Elsevier, Hungary (2008)
24. S.R. Elliott, *J. Non-Cryst. Solids*, 170 (1994) 97
25. J.C. Maxwell, *Treaties on Electricity and Magnetism*, Clarendon, Oxford (1892)